Highly uniform wafer-scale synthesis of -MoO_3 by plasma enhanced chemical vapor deposition

2017 Nanotechnology 28 175601

(http://iopscience.iop.org/0957-4484/28/17/175601)

IOP Publishing Nanotechnology
Nanotechnology 28 (2017) 175601 (6pp) https://doi.org/10.1088/1361-6528/aa67d1

Highly uniform wafer-scale synthesis of α-MoO_3 by plasma enhanced chemical vapor deposition

Hyeong-U Kim[1,5], Juhyun Son[2,5], Atul Kulkarni[2], Chisung Ahn[3], Ki Seok Kim[4], Dongjoo Shin[2], Geun Yong Yeom[1,4] and Taesung Kim[1,2]

[1] SKKU Advanced Institute of Nanotechnology (SAINT), Sungkyunkwan University, Suwon, Republic of Korea
[2] School of Mechanical Engineering, Sungkyunkwan University, Suwon, Republic of Korea
[3] Institute of Advanced Machinery and Technology, Sungkyunkwan University, Suwon, Republic of Korea
[4] School of Advanced Materials Science and Engineering, Sungkyunkwan University, Suwon, Republic of Korea

E-mail: tkim@skku.edu

Received 4 December 2016, revised 24 February 2017
Accepted for publication 15 March 2017
Published 3 April 2017

Abstract

Molybdenum oxide (MoO_3) has gained immense attention because of its high electron mobility, wide band gap, and excellent optical and catalytic properties. However, the synthesis of uniform and large-area MoO_3 is challenging. Here, we report the synthesis of wafer-scale α-MoO_3 by plasma oxidation of Mo deposited on Si/SiO_2. Mo was oxidized by O_2 plasma in a plasma enhanced chemical vapor deposition (PECVD) system at 150 °C. It was found that the synthesized α-MoO_3 had a highly uniform crystalline structure. For the as-synthesized α-MoO_3 sensor, we observed a current change when the relative humidity was increased from 11% to 95%. The sensor was exposed to different humidity levels with fast recovery time of about 8 s. Hence this feasibility study shows that MoO_3 synthesized at low temperature can be utilized for gas sensing applications by adopting flexible device technology.

Supplementary material for this article is available online

Keywords: MoO_3, plasma enhanced chemical vapor deposition (PECVD), wafer-scale, Raman spectroscopy, humidity sensor

(Some figures may appear in colour only in the online journal)

1. Introduction

Two-dimensional (2D) materials have attracted immense attention owing to their unique chemical and physical properties [1]. For example, graphene, the first 2D atomic crystal, possesses excellent material properties such as mechanical stiffness, strength, elasticity, high electrical and thermal conductivities [2]. However, graphene lacks semiconducting characteristics because of its zero band gap. In the past few years, it has been revealed that transition metal dichalcogenides can replace graphene owing to their tunable band gap. Especially, MoS_2 has a tunable band gap, which can be tuned from an indirect (1.29 eV) to a direct (1.90 eV) band gap depending on the number of layers. However, it has a low carrier mobility despite its tunable band gap [3]. On the other hand, 2D semiconducting metal oxides (e.g., molybdenum oxide (MoO_3)) have high dielectric constant (high-k), high electron mobility [4], and a wide band gap (3.2 eV). Moreover, MoO_3 is relatively abundant in nature and shows optical and catalytic properties.

2D material synthesis methods are classified into physical and chemical methods. Mechanical exfoliation is a typical physical method, which yields 2D materials with high quality and small size. Chemical vapor deposition (CVD) is a popular

[5] These authors contributed equally.

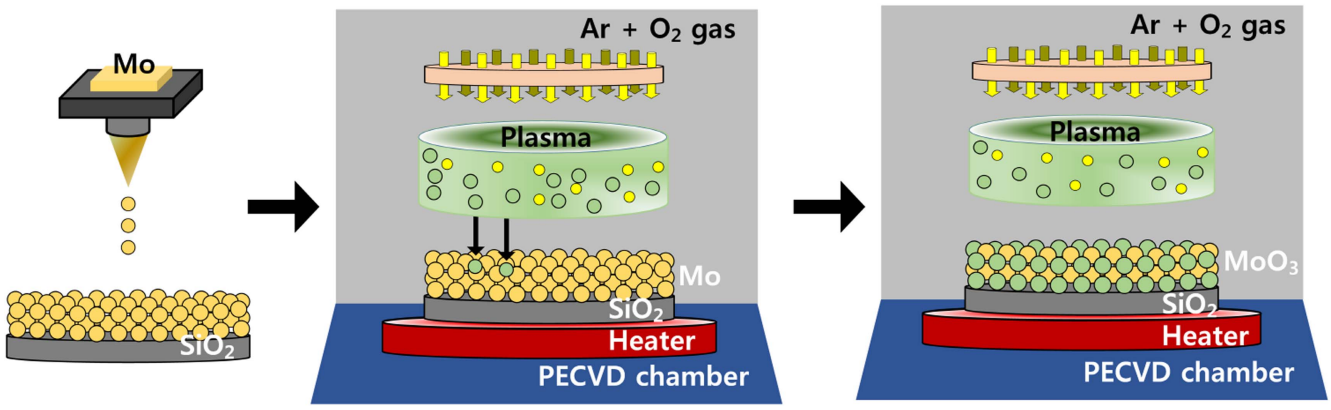

Figure 1. Synthesis processes of MoO_3 in PECVD chamber.

chemical method for the synthesis of uniform and large-area thin films. Graphene can be introduced a band gap by nanoribbons but the required complex synthesis processes with significant loss in carrier mobility [5]. Therefore, layered materials (such as MoO_3 and MoS_2) synthesized by various types of CVD using different types of sources and precursors have been reported to be potential alternatives to graphene [6]. However, the synthesis of these layered materials is a time-consuming process and requires high temperatures (>500 °C). To overcome this problem, the atmospheric pressure CVD technology was reported for the preparation of transition metal oxide thin films at low temperature [7] and also metal organic CVD has been developed for the synthesis of MoS_2 thin films. In this method, two source gases [8] and a precursor film with one source gas are used for reducing the process temperature [9]. On the other hand, plasma enhanced CVD (PECVD) is used for the synthesis of MoS_2 thin films at low temperatures (<300 °C) [10].

Because 2D materials have high surface to volume ratio, they can exhibit superior sensing properties. Various other metal oxide nanocomposite were applied for gas sensing. However, in general they respond to gases at elevated temperatures ~300 °C [11]. Hence not suitable for the flexible substrate based gas sensors, because these sensor operating temperatures are higher than melting point of polymer flexible substrate. In order to meet this requirement, low temperature synthesis of thin and uniform metal oxides film were necessary.

In this study, we carried out, for the first time, the wafer-scale synthesis of α-MoO_3 on Si/SiO_2 by using an inductively coupled PECVD system at low temperature at 150 °C. The structure and uniformity of the synthesized wafer-scale α-MoO_3 were investigated by Raman spectroscopy and transmission electron microscopy (TEM). In addition, a hypothetical mechanism for the formation of α-MoO_3 from Mo by the plasma process is proposed. The humidity sensor was fabricated by depositing Ti/Au electrodes with the help of e-beam evaporator on as-synthesized α-MoO_3 by PECVD. Further, the MoO_3 sensor devices were evaluated for various relative humidity (RH) ranging from 11% to 95%.

2. Experimental

The wafer-scale MoO_3 was synthesized using an inductively coupled plasma source (ICP)–CVD system. The details of ICP–CVD are provided in supplementary figure S1, available online at stacks.iop.org/NANO/28/175601/mmedia. The process of oxidation of Mo was illustrated in figure 1. Initially, a thin layer of Mo (with a thickness of up to 30 nm) was deposited on 4 inch Si/SiO_2 (where SiO_2 thickness is 300 nm) wafer by an e-beam evaporator at a rate of 0.1–1 Å s^{-1} under high vacuum conditions. The Mo-deposited Si/SiO_2 wafer was then loaded in the PECVD system. Inert conditions were achieved by creating a 10^{-6} Torr vacuum and by introducing argon (Ar) (for approximately 10 min) in the system to remove the unwanted impurity residues present on the Mo-deposited Si/SiO_2 wafer. The Mo-deposited Si/SiO_2 wafer was then heated up to 150 °C in the Ar atmosphere. After attaining the desired temperature, the Mo-deposited Si/SiO_2 wafer was treated with H_2 gas plasma for about 10 min to remove the native oxide film on the wafer and to avoid the effect of other contaminants. Finally, to synthesize the wafer-scale MoO_3, Ar (carrier gas) and O_2 (source gas) were introduced into the PECVD system under ultra-high vacuum conditions, and the plasma was generated by controlling the conditions such as, the chamber pressure (100 mTorr), plasma power (550 W), flow rate of the Ar gas (10 sccm) and O_2 gas (10 sccm). The detailed process was depicted in online supplementary figure S2. The synthesized MoO_3 thin film was characterized by Raman spectroscopy (Alpha300 M+, WITec GmbH, Germany) at a wavelength of 532 nm and a laser power of 2 mW, high-resolution transmission electron microscopy (HR-TEM, JEOL-JEM ARM 200 F, Japan), and energy dispersive spectrometry (EDS). The chemical composition was measured by x-ray photoelectron spectroscopy (XPS, MultiLab 2000, Thermo VG, UK) with Mg Ka source. During the XPS measurement, to observe the Mo/O ratio, the take-off angle of the MoO_3 sample was maintained at 45°.

The sensor device structure and setup are illustrated in online supplementary figure S3. The humidity sensor was fabricated with a printed Ti(5 nm)/Au(50 nm) electrode by e-beam evaporation on MoO_3. The humidity sensing

performance of the MoO_3-based sensors were determined by measuring current using semiconductor characterization system (KEITHLEY 4200-SCS) in real time. Water vapor was injected using an atomizer into the chamber. The RH level was controlled with a two channel mass flow controller at 1 l min^{-1}, one for water vapor and one for dry air. The low capacity vacuum pump was connected to outlet of the chamber at 1 l min^{-1}. The RH level in chamber was measured by hygrometer, which is placed near the sensor device under test. When the sensor response reached a saturated value for set RH level, the inlet was closed for removing the humidity in the chamber. All measurements were carried out at room temperature (18 °C–21 °C) at different level of RH. The response time and recovery time are defined on the basis of the time required for the sensor to achieve 90% of the total current change.

3. Result and discussion

The wafer-scale MoO_3 obtained by PECVD of the Mo deposited Si/SiO_2 wafer was characterized by Raman spectroscopy, XPS, HR-TEM, and EDS.

Figure 2(a) shows the Raman spectrum of the synthesized wafer-scale MoO_3 at an excitation wavelength of 532 nm and in the 100–1100 cm^{-1} range. The obtained peaks correspond to the vibration of the ordered structure of MoO_3. The peaks observed at 300, 671, 821, and 999 cm^{-1} correspond to the characteristic peaks of MoO_3. The band at 300 cm^{-1} (B_{2g}, B_{3g}) is attributed to the Mo_3–O bending mode. The band at 671 cm^{-1} (B_{2g}, B_{1g}) is attributed to the asymmetric stretching of the triply connected bridge-oxygen Mo_3–O bridge entity along the *c*-axis. This bridge-oxygen Mo_3–O bridge entity was formed by edge sharing of oxygen (Mo_3–O) with the three adjacent octahedra. The 821 cm^{-1} (A_g, B_{1g}) band was observed only under the 30 nm condition and corresponded to the symmetric stretching of the terminal oxygen atoms or the doubly connected bridge-oxygen Mo–O–Mo entity. Mo–O–Mo was formed by corner sharing of oxygen with two octahedra. The 999 cm^{-1} (A_g, B_{1g}) band corresponds to the symmetric stretching of the terminal oxygen atoms ($Mo^{6+} = O$), which are responsible for the layered structure of α-MoO_3 [12, 13]. β-MoO_3 shows two major vibrational bands at 775 and 850 cm^{-1} [14]. However, these peaks were not observed in the PECVD-synthesized MoO_3, as seen from figure 2(a). Further, the wafer-scale uniformity of the synthesized MoO_3 was investigated by obtaining the Raman spectra at three different locations (figure 2(b)). Moreover, for Raman mapping three peaks were selected 671 cm^{-1} (Mo_3–O), 821 cm^{-1} (Mo_2–O) and 999 cm^{-1} (Mo = O) as shown in figure S4. It is observed that all the three peaks show uniformity in the 20 × 20 μm^2 mapping area. The Raman spectra and mapping clearly reveal that MoO_3 was deposited uniformly on the wafer. The chemical bonding state and surface composition of the synthesized MoO_3 were investigated by XPS. The XPS scans for Mo and O binding energies of the MoO_3 layer are shown in figure 2(c). The Mo $3d_{5/2}$ and $3d_{3/2}$ peaks were observed at 234.0 and 237.2 eV, respectively. The energy difference between the $3d_{5/2}$ and $3d_{3/2}$ peaks was 3.2 eV. The low binding energy component located 533.2 eV (O 1s) (figure 2(d)) originated from the lattice oxygen of MoO_3. The atomic ratio of Mo to O was 1:3.10 and it is very similar with stoichio-metrically expected ratio value of 3. Additionally, Mo and O binding energy were compared for their actual intensity as depicted in online supplementary figure S5. Thus, the XPS results confirmed that MoO_3 was successfully synthesized [15].

The structure of the synthesized MoO_3 was further investigated by HR-TEM. Figure 2(e) shows the cross-section image obtained by exposing the MoO_3 sample to a focused ion beam (FIB). The inset shows the EDS spectrum of MoO_3 (30 nm Mo condition). The EDS analysis confirmed the presence of O and Mo atoms (denoted by yellow circles). The stoichiometric ratio (Mo:O) estimated from the EDS spectrum was close to 3. The result further confirmed the formation of MoO_3. The preferential (100) orientations of MoO_3 shown in figure 2(f) were used to determine the lattice spacing of the synthesized MoO_3 with bright field mode of the scanning TEM (STEM) mode. The lattice spacing was similar to that reported for MoO_3 in previous reports. A lattice spacing of 0.38 nm was obtained, corresponding to the (100) plane of the orthorhombic phase of MoO_3 [12].

Previous studies, PECVD are used to deposit by the adsorption and reaction of dissociated gases with precursors on the substrate [16]. In this study, a Mo film was deposited on the Si/SiO_2 substrate and the resulting Mo-deposited Si/SiO_2 was used as the precursor. The precursor was then oxidized by O_2 for the synthesis of MoO_3. We have used this technique in our previous studies for the synthesis of MoS_2 thin films [10, 17]. The mechanism for the synthesis of wafer-scale MoO_3 is illustrated in figure 3. During the plasma activation, the Ar gas present in the chamber was ionized. Herein, the specific reason to use Ar is to produce more oxygen ions in the sheath area of plasma, this can further help to penetrate O_2 plasma into the 30 nm thick Mo film to achieve MoO_3.

This ionization of Ar gas led to a charge transfer reaction between the resulting Ar ions and O_2 because of collision. This collision resulted in the conversion of O_2 to O_2^+, and a sheath layer was formed above the Mo-deposited wafer. As O_2^+ carried a positive charge and the Mo wafer was chargeless (i.e. it was grounded), an electric field was generated and O_2^+ reacted with Mo on the Si/SiO_2 substrate. Because of this reaction, it was possible to oxidize Mo at a low temperature (i.e. 150 °C). Further, this reaction continued for approximately 90 min to finally yield MoO_3 on the Si/SiO_2 wafer [18].

The dependence of current versus RH is shown in figure 4. The sensing characteristics of the optimized MoO_3 film device were measured current change by increasing or decreasing RH at the room temperature. It is reported that, the water molecule acts as an electron donor (n-type doping), hence with the exposure of RH, the Fermi level of MoO_3 shifted toward the conduction band by decreasing the resistance of MoO_3, resulting in increase in the current [19]. It is obvious that the

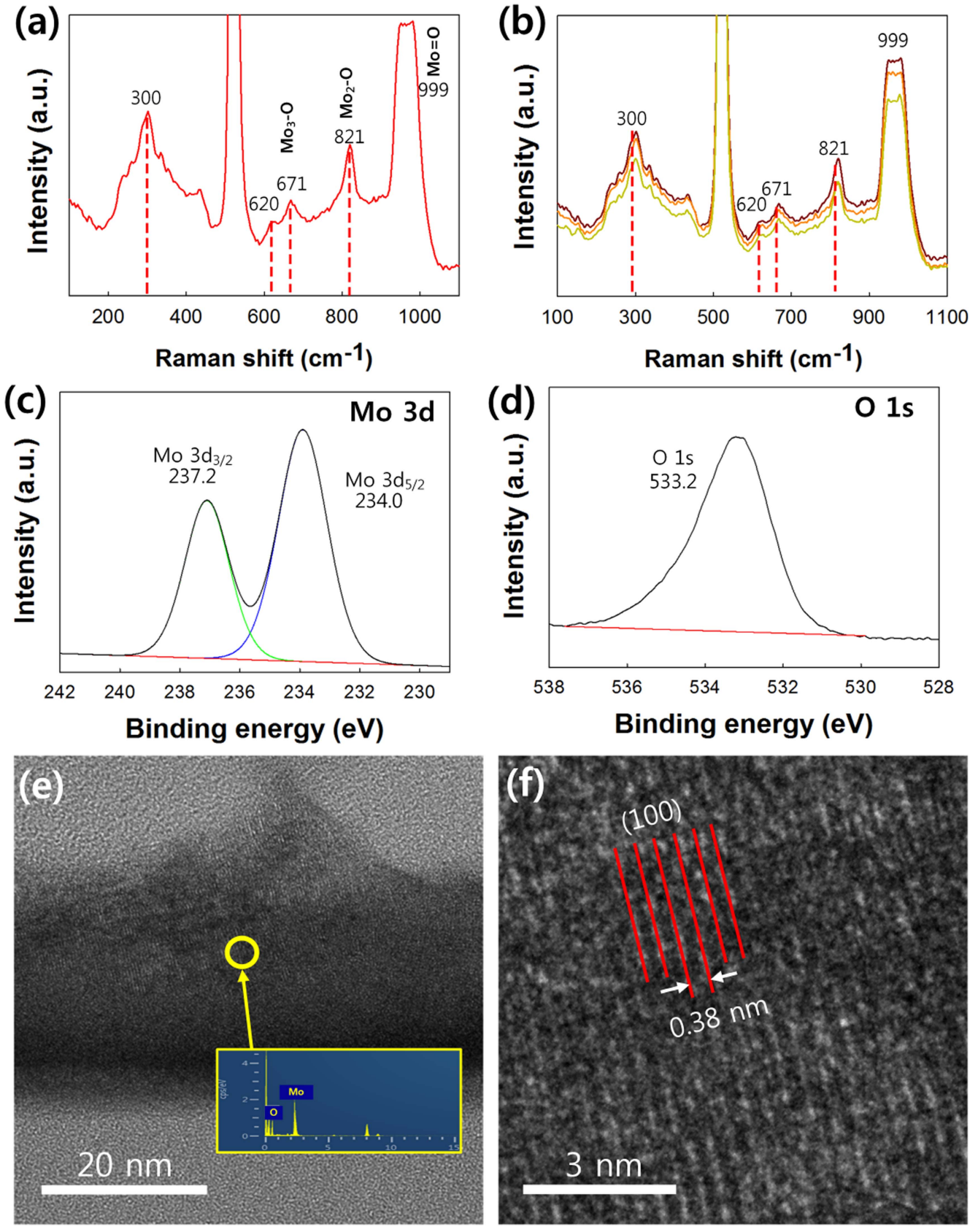

Figure 2. (a) Raman spectra of MoO_3 (for 30 nm Mo condition). (b) Raman spectra of three points on the synthesized MoO_3 (for 30 nm Mo condition). (c) XPS spectra of Mo 3d. (d) O 1s spectrum (for 30 nm Mo condition). (e) TEM cross-section image of the sample obtained by exposing the sample to a FIB; the inset shows the EDS spectrum of MoO_3. (f) STEM mode image of MoO_3.

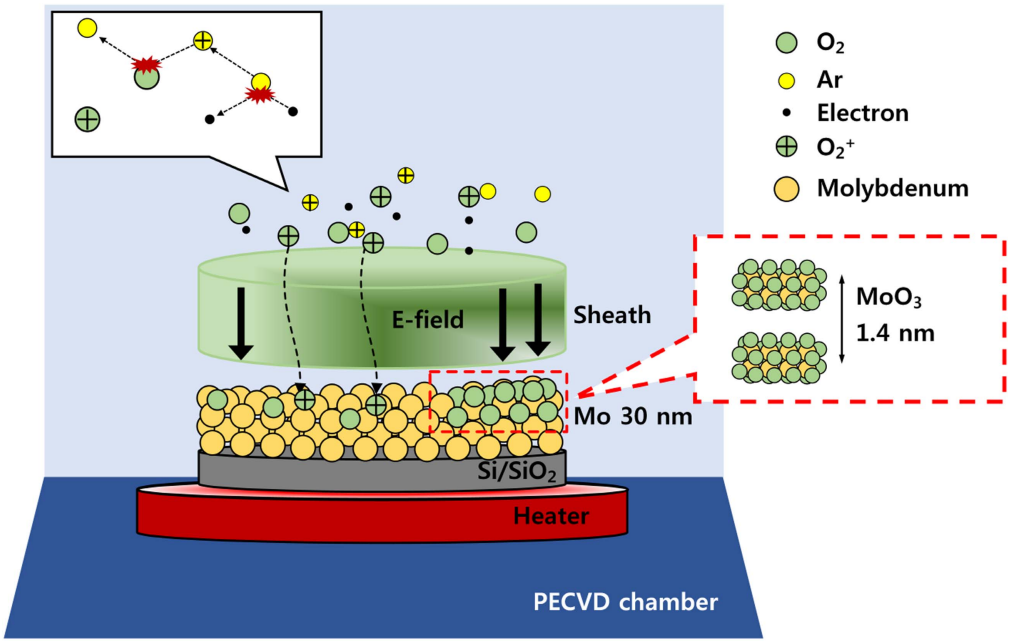

Figure 3. Schematic of the synthesis of MoO_3 on Si/SiO_2, showing the film formation mechanism.

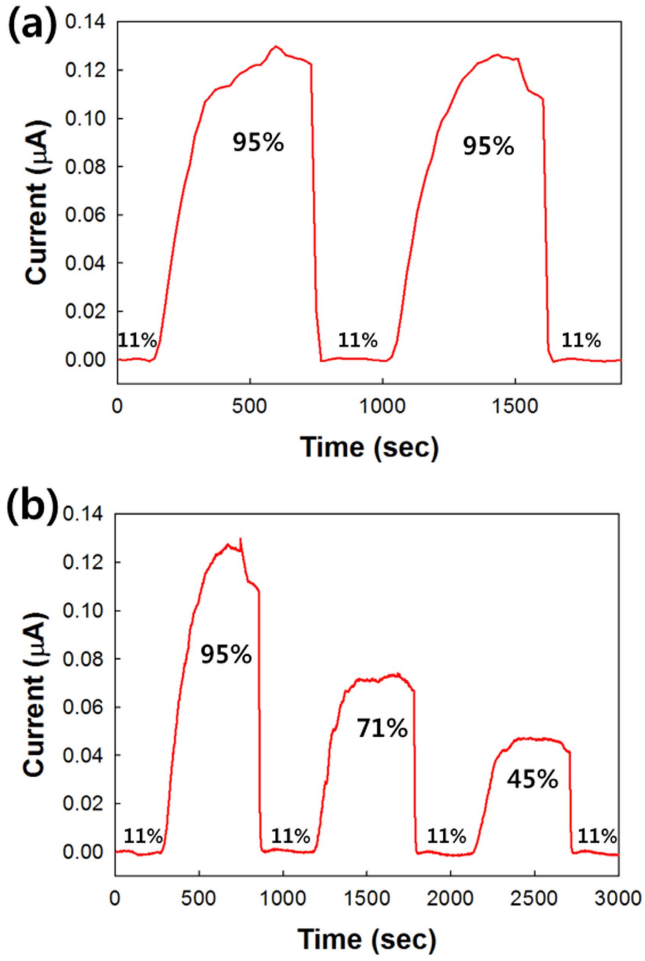

Figure 4. A typical current–time plot of the MoO_3-based RH sensor. (a) Response of the sensor during the RH switching between 11% and 95% for repeated cycles. (b) RH sensing response at different humidity levels at room temperature.

Table 1. The comparative data of various kinds of nanomaterials with MoO_3 film related to response/recovery time.

Material	Type	Response time	Recovery time	References
CuO	NW	120	120	[19]
SnO_2	NW	120–170	20–60	[20]
TiO_2	Nanotube	100	190	[21]
MoO_3	Film	175	8	Present work

response and recovery behavior is one of the most important characteristics for evaluating the performance of humidity sensors. The stability of the MoO_3 gas sensor was checked with two cycles. The stability of the sensor was performed in conjugative cycles between two RH levels, by increasing the RH from 11% to 95%, as shown in figure 4(a). It is observed that, for RH 95%, the response and recovery time are ∼195 and ∼15 s, respectively. Figure 4(b) presents the current–time plot obtained by exposing the MoO_3 sensor to the RH level such as 95%, 71%, and 45% and returned to low humidity level of 11%. At low humidity (11% RH), only a few water molecules will be present. At 71% RH, the response time and recovery time were ∼185 s and ∼11 s, respectively. At a lower RH of 45%, the response time and recovery time were ∼175 s and ∼8 s, respectively. As observed, the sample had a quick recovery to the RH change. Table 1 shows the comparative results for various kinds of metal oxide nanostructures with different morphology, in terms of response time and recovery time, for comparing the performance of the humidity sensor fabricated in this study [20–22]. For the MoO_3 sensor fabricated in this study, the recovery time was very low because the adsorbed water molecules desorbed quickly during humidity decrease from high to low levels. Hence, low temperature

synthesized MoO_3 can be suitable candidate for the sensitive humidity/gas sensor application and can be applied flexible device technology.

4. Conclusions

In the present study, wafer-scale α-MoO_3 was successfully synthesized on a Si/SiO_2 wafer using a PECVD system at 150 °C. To the best of our knowledge, this is the first attempt made till date to synthesize wafer-scale MoO_3 at such a low temperature. The synthesized α-MoO_3 characterization by Raman spectroscopy, HR-TEM, XPS, and EDS confirms the successful synthesis which are comparable to other synthesis methods. The Raman spectroscopy results revealed that the α-MoO_3 was deposited uniformly on the Si/SiO_2 wafer. The synthesized α-MoO_3 responded well for the RH from 11%–95%. Hence this feasibility study shows that MoO_3 synthesized at low temperature can be utilized for the gas sensing applications by adopting flexible device technology.

Acknowledgments

This work was supported by the International S&T Cooperation Program of China (ISTCP) (2014DFG52760) and NRF-2013K1A3A1A20046951. This work was also supported by a National Research Foundation of Korea (NRF) grant funded by the Korean government (NRF-2015R1D1A1A01057861).

References

[1] Bonaccorso F *et al* 2010 Graphene photonics and optoelectronics *Nat. Photon.* **4** 611–22
[2] Geim A K and Grigorieva I V 2013 Van der Waals heterostructures *Nature* **499** 419–25
[3] Lee C *et al* 2010 Anomalous lattice vibrations of single-and few-layer MoS_2 *ACS Nano* **4** 2695–700
[4] Balendhran S *et al* 2013 Enhanced charge carrier mobility in two-dimensional high dielectric molybdenum oxide *Adv. Mater.* **25** 109–14
[5] Jiao L *et al* 2010 Facile synthesis of high-quality graphene nanoribbons *Nat. Nanotechnol.* **5** 321–5
[6] Jeon J *et al* 2015 Layer-controlled CVD growth of large-area two-dimensional MoS_2 films *Nanoscale* **7** 1688–95
[7] Gesheva K *et al* 2014 APCVD transition metal oxides—functional layers in 'smart windows' *J. Phys.: Conf. Ser.* **559** 012002
[8] Mun J *et al* 2016 Low-temperature growth of layered molybdenum disulphide with controlled clusters *Sci. Rep.* **6** 21854
[9] Lee Y *et al* 2014 Synthesis of wafer-scale uniform molybdenum disulfide films with control over the layer number using a gas phase sulfur precursor *Nanoscale* **6** 2821–6
[10] Ahn C *et al* 2015 Low-temperature synthesis of large-scale molybdenum disulfide thin films directly on a plastic substrate using plasma-enhanced chemical vapor deposition *Adv. Mater.* **27** 5223–9
[11] Galatsis K *et al* 2001 Semiconductor MoO_3–TiO_2 thin film gas sensors *Sensors Actuators* B **77** 472–7
[12] Kalantar-Zadeh K *et al* 2010 Synthesis of nanometre-thick MoO_3 sheets *Nanoscale* **2** 429–33
[13] Lupan O *et al* 2014 Versatile growth of freestanding orthorhombic α-molybdenum trioxide nano-and microstructures by rapid thermal processing for gas nanosensors *J. Phys. Chem.* C **118** 15068–78
[14] Haro-Poniatowski E *et al* 1998 Laser-induced structural transformations in MoO_3 investigated by Raman spectroscopy *J. Mater. Res.* **13** 1033–7
[15] Lee Y J *et al* 2009 Chemical vapour transport synthesis and optical characterization of MoO_3 thin films *J. Phys. D: Appl. Phys.* **42** 115419
[16] Kim H *et al* 2013 Synthesis of MoS_2 atomic layer using PECVD *ECS Trans.* **58** 47–50
[17] Kim H-U *et al* 2015 *In situ* synthesis of MoS_2 on a polymer based gold electrode platform and its application in electrochemical biosensing *RSC Adv.* **5** 10134–8
[18] Floquet N *et al* 1992 Structural and morphological studies of the growth of MoO_3 scales during high-temperature oxidation of molybdenum *Oxid. Met.* **37** 253–80
[19] Anderson J H Jr and Parks G A 1968 Electrical conductivity of silica gel in the presence of adsorbed water *J. Phys. Chem.* **72** 3662–8
[20] Wang S-B *et al* 2012 CuO nanowire-based humidity sensor *IEEE Sens. J.* **12** 1884–8
[21] Kuang Q *et al* 2007 High-sensitivity humidity sensor based on a single SnO_2 nanowire *J. Am. Chem. Soc.* **129** 6070–1
[22] Zhang Y *et al* 2008 Synthesis and characterization of TiO_2 nanotubes for humidity sensing *Appl. Surf. Sci.* **254** 5545–7